NASA Technical Memorandum 109008

Active Control of Fan-Generated Plane Wave Noise

Carl H. Gerhold, William E. Nuckolls, Odilyn L. Santa Maria, and Scott D. Martinson

August 1993

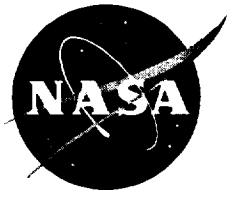

National Aeronautics and Space Administration

Langley Research Center
Hampton, Virginia 23681-0001

ACTIVE CONTROL OF FAN-GENERATED PLANE WAVE NOISE

ABSTRACT

An experiment is reported in which the noise generated by a ducted fan is controlled by a time domain active adaptive noise control system. The control sound source consists of loudspeakers arranged in a ring around the fan duct. The error sensor location is in the fan duct. The purpose of this experiment is to verify previous research on control of lower order mode fan generated noise; and to demonstrate that the in-duct error sensor reduces the mode spillover in the far field, thereby increasing the efficiency of the control system. In this first series of tests, the number of rotors and stators is the same so that predominantly plane waves are generated. The control system is found to reduce the blade passage frequency tone significantly in the acoustic far field when the mode orders of the noise source and of the control source are the same; in the case discussed, when they are both plane waves. The noise reduction is not as great when the source is generating plane waves while higher order modes are present in the duct even though the modes are evanescent, but the control system still converges stably and global noise reduction is demonstrated in the far field. The control system is found to be stable and to reduce the sound level radiated from the duct for fan speeds for which the first radial mode is generated. Further experimentation is planned in which the performance of the system will be evaluated when higher order radial and spinning modes are generated.

ACTIVE CONTROL OF FAN-GENERATED PLANE WAVE NOISE

INTRODUCTION

In order for the American commercial airplane industry to remain competitive in the international marketplace, it must continue its leadership role in technological development, of which noise control is an increasingly significant element. The emergence of the ultra-high bypass ratio engine on aircraft in the 21st century is expected to shift the dominant engine noise source from the jet to the fan. The blade tip speed will be subsonic or transonic so that the fan noise will have high tonal content at harmonics of the blade passage frequency and the fundamental tone will be at a frequency less than 1000 Hz. In order to provide sufficient thrust, the engine diameter will be on the order of 12 feet and, in fact, engine size will be limited by considerations such as space available under the wing and allowable landing gear length. Safety and noise considerations have led to development of designs with a nacelle surrounding the fan. Weight is a significant parameter in the design of the power plant and in order to minimize the weight of the large diameter nacelle, it will be as short and as thin as possible. The thickness and length restrictions limit the amount of passive noise control treatment that can be applied, while the relatively low blade passage frequency necessitates thick bulk liner treatment which is extensive in the axial direction.

The conflicting goals of minimum weight and maximum noise reduction can be aided materially by active noise control. Active noise control is well suited for applications in which a low frequency noise source limits the utility of passive control methods (Chaplin, 1983). An active noise control system can provide significant noise reduction without excessive weight penalty, and research is continuing on development of lightweight, efficient control sound sources (Dungan, 1992).

Noise in ducts has long been considered an attractive application of active noise cancellation because the duct serves as a waveguide both to the source noise and to the control sound. Paul

Lueg was issued a patent nearly 60 years ago for control of sound in a long duct using a system that consists of a reference microphone to measure the noise to be controlled, a source for the control sound which is equal in amplitude but opposite in phase with the noise at that point, and a processor that delays to adjust for propagation from the measurement microphone to the control source (Lueg, 1936). Two problems have delayed implementation of this control concept. One is development of the processor, which has now become widely available through the technologies of the digital signal processor chip and the personal digital computer. The other problem is the instability that is caused by feedback of the control signal onto the reference microphone. To control this, one research area takes the direction of development of sound sources that are intended to generate sound that propagates in one direction from the control source, thus reducing the feedback (Swinbanks, 1973). Another direction is to develop a model of the feedback loop in the digital signal processor and to subtract the synthesized feedback signal from the measured reference signal (Eriksson et al, 1989). A third method to control the instability is to eliminate feedback altogether by using a non-acoustic reference, such as the signal from a tachometer on an engine operating at steady state (Eghtesadi and Chaplin, 1987). Utilization of the non-acoustic reference is appropriate when the source noise is periodic, such as is generated by a fan, and when the controller needs only frequency information about the source. The control system described in this paper uses a non-acoustic reference signal from a blade passage sensor on the fan.

Active noise control systems have been shown to reduce multiple harmonic tones of periodic noise generated in a duct by a loudspeaker (Tichy et al, 1984). Numerous researchers have demonstrated control of duct-borne sound generated by fans, either multiple pure tones (Ffowcs Williams, 1981, Koopman et al, 1988), or broadband fan noise (Eriksson et al, 1989). The results reported generally show the noise reduction at the error microphone where the cancellation is expected to be quite effective. Researchers at Virginia Polytechnic Institute and State University have developed

an active control system on the inlet of a commercial jet engine using a ring of loudspeakers as the control source (Thomas et al, 1993). The error microphones, which are located in the acoustic far field for the experiments with this engine, have a large diaphragm so that the sound is effectively integrated over a finite space. The result is a broadened spatial extent of noise reduction with a slight loss in magnitude. The most significant problem encountered in this experiment is the mode-spillover due to mismatch of the mode compositions of the noise and the control sources. This mode spillover results in noise amplification at some locations away from the control microphones.

The purpose of the experiment reported in the present paper is to develop a control system utilizing error sensors located in the fan duct. It is felt that the spatial extent of noise reduction and, more importantly, the mode spillover effect, can be controlled more effectively with the in-duct error sensor.

CONTROL THEORY

This section discusses the general theoretical development of the Least Mean Square (LMS) Algorithm and the Adaptive Filter. The block diagram of the generalized control system is shown in figure 1. The block labeled "PLANT" indicates a transfer function in which some measurable continuous signal s is the input and the output is a disturbance signal d. The control system signified by the dashed lines generates a discretized signal y_k which combines with the disturbance to produce an error ε. It is the purpose of the control system to generate the signal which minimizes the error.

The continuous signal, s, is sampled at discrete time intervals, Δ, in the digital computer and collected into a vector $\mathbf{X}_k$ of length n:

$$\mathbf{X}_k = \begin{Bmatrix} x_k \\ x_{k-1} \\ \cdot \\ \cdot \\ \cdot \\ x_{k-n+1} \end{Bmatrix}$$

The element x_k is the digitized sample of s taken at the present time. The element x_{k-1} is the digitized sample of s taken on the previous loop, Δ seconds in the past, and so on to x_{k-n+1} which is the digitized sample of s taken $(n-1)^*\Delta$ seconds in the past. The vector $\mathbf{X}_k$ is constantly updated on each loop with the oldest value discarded, and the newest value put in the top of the array. The scalar output of the adaptive filter is obtained from:

$$y_k = \sum_{l=0}^{n-1} w_l x_{k-l} = \mathbf{W}^T \mathbf{X}_k \qquad (1)$$

where:

$\mathbf{W}^T$ = the transpose of the vector $\mathbf{W}$ and

$\mathbf{W}$ = a vector of weighting coefficients;

$$= \begin{Bmatrix} w_0 \\ w_1 \\ \cdot \\ \cdot \\ \cdot \\ w_{n-1} \end{Bmatrix}$$

The error at time t_k is the combination of the disturbance and the filter output:

$$\varepsilon = d - \mathbf{W}^T \mathbf{X}_k \qquad (2)$$

The mean square error is:

$$\varepsilon^2 = d^2 - 2\, d\, \mathbf{X}_k^T \mathbf{W} + \mathbf{W}^T \mathbf{X}_k \cdot \mathbf{X}_k^T \mathbf{W} \qquad (3)$$

The minimum mean square error is obtained by setting to zero the derivative of the expectation of the mean square error with respect to the weighting vector (Widrow et al, 1975). The optimum weight vector $\mathbf{W}^*$ is the vector of weight coefficients that produces

the minimum mean square error. It is generally refered to as the Weiner weight vector and it is evaluated from:

$$\mathbf{W}^* = \mathbf{R}^{-1} \cdot \mathbf{P} \tag{4}$$

where:

$\mathbf{R}^{-1}$ = the inverse of the matrix $\mathbf{R}$

$\mathbf{R} = E[\mathbf{X}_k \cdot \mathbf{X}_k^T]$

$\mathbf{P} = E[d\,\mathbf{X}_k]$

E = the Expectation operator

The LMS Algorithm is intended to approximate the optimum solution, expression 4, in real time, using the method of steepest descent. The weight function for the current loop through the controller, $\mathbf{W}_j$ is updated using the weight function from the previous pass through the loop, $\mathbf{W}_{j-1}$ plus a change proportional to the negative gradient of the mean square error, ∇_j

$$\nabla_j = \begin{Bmatrix} \frac{\partial(\varepsilon_k^2)}{\partial w_0} \\ \bullet \\ \bullet \\ \bullet \\ \frac{\partial(\varepsilon_k^2)}{\partial w_{n-1}} \end{Bmatrix} = 2\,\varepsilon_k \begin{Bmatrix} \frac{\partial(\varepsilon_k)}{\partial w_0} \\ \bullet \\ \bullet \\ \bullet \\ \frac{\partial(\varepsilon_k)}{\partial w_{n-1}} \end{Bmatrix} \tag{5}$$

where:

ε_k = the current value of the digitized sample of the error

The slope of the error curve is evaluated from expression 2:

$$\begin{Bmatrix} \frac{\partial(\varepsilon_k)}{\partial w_0} \\ \bullet \\ \bullet \\ \bullet \\ \frac{\partial(\varepsilon_k)}{\partial w_{n-1}} \end{Bmatrix} = \mathbf{X}_k \qquad (6)$$

The weighting vector is updated in the LMS Algorithm according to the expression:

$$\mathbf{W}_j = \mathbf{W}_{j-1} - 2\,\mu\,\nabla_j$$

$$= \mathbf{W}_{j-1} + 2\,\mu\,\varepsilon_k\,\mathbf{X}_k \qquad (7)$$

where:

μ = user defined adaptation constant

The algorithm will converge in the mean and will be stable as long as the adaptation constant μ is positive and less than the reciprocal of the largest eigenvalue of the matrix **R** (Widrow et al, 1975). The speed with which the algorithm converges is dependent on the adaptation coefficient and the convergence is greatest for the largest value of μ that does not violate the maximum value criterion. The expected value of the weight vector in expression 7 converges to the Weiner weight vector, expression 4, when the input vectors are uncorrelated over time.

EXPERIMENT LAYOUT

Duct

The experimental setup consists of a duct with the following major elements: inflow control device, control hardware section, an axial flow fan, and an anechoic termination. The unit is installed in the laboratory space of the Anechoic Noise Facility at NASA LaRC. The inlet to the fan duct is in the anechoic chamber and the

remainder of the duct is in the model assembly area adjacent to the chamber. Figure 2 shows a schematic of the overall experiment layout. The anechoic chamber volume is 17000 cubic feet and the acoustic wedges on floor, walls, and ceiling are 3 feet deep, giving a lower cut-off frequency of approximately 100 Hz. Far field sound measurements are made using a 1/2" B&K microphone on a rotating boom at a radius of 5 feet from the face of the duct inlet. An inflow control device is installed on the inlet of the duct (Homyak et al, 1983). The purpose of the inflow control device is to straighten flow into the duct and to break up turbulent eddies which may be ingested into the fan. The inflow control device is designed to simulate the uniform inflow of forward flight in a static test (Chestnutt, 1982). Figure 3 is a photograph of the inflow control device on the duct inlet installed in the anechoic chamber. The figure also shows the far field microphone.

The control hardware duct piece contains 24 microphones arranged uniformly around the duct and installed flush with the inside surface of the duct. The error sensors in the control system are taken from among these 24 microphones. The microphones are 1/8" embedded in a threaded 1/2" diameter cannister. Twelve control drivers are distributed around the duct, as shown in the photograph, figure 4. Each driver has input impedance of 16 Ω. and is rated at 120 W rms. The drivers are attached to the duct by transition horns that are thick-walled to prevent sound transmission. The horns transition from the round outlet of the driver to the rectangular slot in the duct wall. The areas of both are the same, so minimum impedance mismatch is expected. A thin wire mesh covers the slot on the inside surface of the duct to reduce cavity resonance as a source of noise.

The fan, whose outer casing is shown in figure 4, is designed to generate noise predominantly by the interaction of the rotor wake with the downstream stator. The fan unit consists of a 16 bladed rotor with airfoil-shape blades that are designed to deliver 3 lb/sec air flow and to produce 5 pounds thrust at 4500 rpm. The stator vanes can be positioned from 0.5 to 3.0 blade chord lengths downstream of the rotor. The purpose for the variability is to

investigate the effect of rotor/stator spacing on fan noise. Provision is made for flow disturbance rods or other flow control devices to be positioned upstream of the rotor, although none are installed for this test. The fan tip diameter is 11.81" with a hub diameter of 6". The fan is driven by a 3 HP electric motor and rotor speeds up to 6000 rpm can be achieved. The blade passage frequency can thus be up to 1600 Hz. This frequency corresponds to wavenumber normalized by duct radius, ka = 4.38 for the 11.81" diameter duct. The normalized wavenumber value indicates that, in addition to the plane wave, the duct can support the first two circumferential (spinning) modes with the lowest order radial mode, ka = 1.84 and ka = 3.05; and the first radial mode with the lowest order circumferential mode, ka = 3.83, for blade passage frequency tones. It is expected that any higher order modes would not be cut on. Although numerous modes can be cut on in the duct, the mode which is generated into dominance is determined by the number of rotors and stators, according to criteria suggested by Tyler and Sofrin (Tyler and Sofrin, 1962). The fan has been designed so that the number of stator vanes can be 16, 17, or 18 and always uniformly spaced. It is expected that the plane wave will dominate when the fan is configured with 16 stator vanes, the 1^{st} circumferential (spinning) mode will dominate when 17 vanes are installed, and the 2^{nd} circumferential (spinning) mode will dominate with the 18 vane configuration.

The fan is instrumented with static pressure taps upstream of the rotor, at the rotor location, and downstream of the stators. A total pressure rake is located at the stator. Figure 5 shows the pressure performance curve for the fan. The fan is instrumented with two proximity probes, one to provide a signal proportional to the blade passage frequency and one to indicate shaft speed.

A muffler section is located downstream of the fan as shown in figure 2. This 12 foot long duct is lined with perforated metal and two inches of sound absorbing material. The muffler reduces fan noise radiation into the laboratory space and acts as an anechoic termination for the discharge of the fan.

Control System.

The active, adaptive noise control system uses a time domain LMS algorithm. Figure 6 shows the schematic diagram of the control system, which includes the fan and control hardware sections of the duct. The reference signal for the controller is supplied by a proximity probe which gives a signal at each blade passage. The probe signal is low pass filtered to remove the harmonics of the blade passage frequency leaving a tone at the blade passage frequency which is input to the computer. The error signal is the combination of the fan and control noise measured at the error microphones. The signal is band pass filtered, to remove extraneous noise, and amplified before passing into the computer. The output from the computer is the control signal which is passed through up to 12 channels of gain/phase network to adjust the signal to the individual loudspeaker according to the order of the mode being controlled.

The controller is a Digital Signal Processor (DSP) board which is mounted in a personal computer through the ISA bus. The chip used is a Texas Instruments TMS320C30 (C30) floating point DSP with instruction time of 60 nanoseconds. There are 192 Kwords of 32-bit zero wait state static random access memory, along with 64 Kwords of 32-bit one wait state random access memory (RAM), dual ported between the C30 and the ISA bus. The dual port RAM is used to download all of the code to the C30 and to pass data between the personal computer and the C30. The reference and error signals are input to the computer by a 16-bit Analog-to-Digital Converter with a fourth order filter to prevent aliasing. The Analog-to-Digital Converter has 153 KHz throughput and $\pm$ 3 volt input range. The signal is output through a 16-bit Digital-to-Analog Converter with fourth order filter to reconstruct and smooth the digital signal produced by the C30. The Digital-to-Analog Converter has 667 KHz throughput with $\pm$ 3 volt output range.

The control algorithm consists of a 4-coefficient Adaptive Filter which applies the weighting factor to the reference signal to

generate the control signal, and a Least Mean Square algorithm which updates the weighting coefficients using the current values of the coefficients and the error. The whole active, adaptive control system is driven at the the sampling frequency (Δ) of the Analog-to-Digital Converters. Conversions are initiated through an onboard timer which is controlled through software. The processes of obtaining reference and error samples, updating the weighting coefficients, and generating the new control signal are accomplished within Δ. Therefore the efficiency of the algorithm affects the maximum frequency that the DSP can actively control. All the software is coded in assembly language to optimize the efficiency. The current implementation with four coefficients can execute within a Δ of 15 microseconds, which corresponds to 66 KHz.

RESULTS

A series of tests was run with the active, adaptive noise control system incorporated into the fan duct system. The number of stator vanes in the fan is 16 for the tests reported here. This is the same as the number of blades and it ensures that the predominant modes that are generated are those for which the sound pressure phase is uniform around the circumference of the duct. The rotor/stator spacing is set to the minimum value for the greatest rotor/stator interaction for this series of tests. One error microphone in the duct and two control speakers on opposite sides of the duct were activated for the series of tests reported here.

Figure 7 shows the directivity plot of fan noise in the acoustic far field with the fan operating at 1500 rpm. The blade passage frequency at this fan speed is 400 Hz, and the normalized wavenumber, ka, is 1.12. The blade passage frequency is thus below the first spinning mode cut-on, and it is expected that only plane waves will propagate in the duct. The microphone signal has been filtered so that the directivity plot in figure 7 shows the blade passage frequency tone. When the controller is not activated, the directivity plot shows sound radiation that is spatially uniform, confirming the expected plane wave sound propagation in the duct.

When the controller is activated, the curves in the figure indicate that the sound level is reduced in the far field by as much as 24 dB on the fan axis. The noise reduction is seen to be fairly consistent as the observer moves from 0° to 90°. The average reduction of sound level at the in-duct error microphone signal is found to be 26.1 dB with the standard deviation of 1.8 dB. This noise reduction was found to be quite stable throughout the time that it took to complete the test.

The fan was run at 2700 rpm, which corresponds to blade passage frequency of 720 Hz. This frequency is above the first spinning mode cut-on frequency for the duct, but it is expected that the spinning mode would not be cut on strongly in light of the fact that the number of blades and stators is the same. The directivity plots of the blade passage frequency tones for control off and control on are shown in figure 8. The control off directivity curve shows a forward radiating lobe of 60° width. When the controller is activated, the sound level reduction is relatively uniform at 2. dB from the fan axis to 90° to the fan axis. The far field noise reduction, while spatially uniform, is much less than it is when blade passage frequency is below the spinning mode cut-on. This is reflected in the noise reduction at the error microphone, which is 18.8 dB. The controller is stable, maintaining the average attenuation at the error microphone throughout the test with standard deviation of 2.0 dB.

The efficacy of the controller as a function of frequency is indicated in figure 9. This plot was generated by operating the fan at speeds from 500 rpm to 6000 rpm and comparing the blade passage frequency tones at the error microphone for control off with control on at each speed. The control off spectrum for the in-duct error microphone shows a general trend in sound level to go up with engine speed punctuated by a large increase at 4800 rpm and somewhat smaller increases at 2300 rpm and 3700 rpm. These latter increases correspond to cut-on frequencies of the spinning modes (1,0) and (2,0) when corrected for hub-to-tip ratio of 0.5. (Tyler and Sofrin, 1962). The sound level increases at these frequencies are not large because the generation mechanism for the higher order spinning

modes is weak. The cause of the increase in sound level at 4800 rpm, which corresponds to normalized wavenumber, ka = 3.49, is not known at this time since the first radial mode cut-on is not expected until ka = 3.81. When the controller is activated, the system reaches steady state with the error microphone signal decreased at all operating speeds. The noise reduction is from 3 dB to as much as 27 dB. at the error microphone.

Figure 10 shows the spectral noise reduction achieved in the far field on the axis of the duct. When the control is off, the far field spectrum is smoother than it is in the duct, showing that the duct modes are not propagated into the far field. Noise reduction is obtained with the controller at all operating speeds except 2700, 3900, and 5700 rpm. There was not sufficient time in this series of tests to measure the directivity at operating speed above 5240 rpm at which the first radial mode is cut on. However, the spectra in figures 9 and 10 indicate that the controller reduces sound at both the error and the far field microphones at operating speeds above 5240 rpm.

It was found to be necessary to change the sign of the signal out of the controller at certain frequencies. This corresponds to changing the phase of the signal by 180°. The reason that this sign change is necessary is that, at frequencies where the distance from the control speakers to the error microphone corresponds to an odd number of half-wavelengths, the disturbance and control sounds add out of phase from the time the control system first comes on. Thus the combined signals are already at optimum phase difference and it remains only to search for the control signal magnitude to minimize the error. The controller begins changing the coefficients in a search for the minimum combined signal, and in so doing, changes the phase of the control signal. This generally leads to instability. The situation is corrected by reversing the sign of the controller output, so that both the amplitude and the phase of the control signal are not optimized at the beginning of the control cycle.

CONCLUSIONS

The experiments discussed in this paper have verified that time domain active, adaptive control is applicable to reduction of fan noise in a duct. The control system has been applied to tones that are generated at the blade passage frequency. The controller is stable over a range of frequencies in which plane waves and higher order duct modes can propagate. The fan has been configured so that the rotor-stator interaction generates predominantly plane wave modes, but sound measurements in the duct indicate the presence of higher order modes. The system utilizes an in-duct error microphone which is shown to provide global noise reduction in the acoustic far field. The system is especially effective when the mode structures of the noise source and of the control source are the same, in this case when both are plane waves.

REFERENCES

Chaplin, G.B., 1983, "Anti-Noise, the Essex Breakthrough", Chartered Mechanical Engineer, vol. 30, pp 41-47.

Chestnutt, D. ed, 1982, "Flight Effects of Fan Noise", NASA CP-2242.

Dungan, M.E., 1992, "Development of a Compact Sound Source for the Active Control of Turbofan Inlet Noise", MS Thesis, Virginia Polytechnic Institute and State University, Blacksburg, Virginia.

Eghtesadi, K. and Chaplin, G.B., 1987, "The Cancellation of Repetitive Noise and Vibration by Active Methods", proceedings of NOISE-CON '87, State College, Pennsylvania, pp 347-352 .

Eriksson, L.J., Allie, M.C., Bremigan, C.D., and Gilbert, 1989, J.A., "Active Noise Control on Systems with Time-Varying Sources and Parameters", Sound and Vibration, vol 23, no 7, pp-16-21.

Ffowcs Williams, J.E., 1981, "The Silent Noise of a Gas Turbine", Spectrum, British Science News, vol. 175, no. 1.

Homyak, L., McArdle, J.G., and Heidelberg, L.J., 1983, "A Compact Inflow Control Device for Simulating Flight Fan Noise", AIAA paper no. 83-0680.

Jessel, M.J., and Mangiante, G., 1972, "Active Sound Absorbers in an Air Duct", Journal of Sound and Vibration, vol 23. pp 383-390.

Koopman, G.H., Fox, D.J., and Niese, W., 1988, "Active Source Cancellation of the Blade Tone Fundamental and Harmonics in Centrifugal Fans", Journal of Sound and Vibration, vol 126, pp 209-220.

Lueg, P., 1936, " Process of Silencing Sound Oscillations", U.S. Patent number 2,043,416.

Swinbanks, M.A., 1973, "The Active Control of Sound Propagation in Long Ducts", Journal of Sound and Vibration, vol. 27, 411-436.

Tichy, J., Warnacha, G.E., and Pool, L.A., 1984, "Active Noise Reduction Systems in Ducts", ASME paper no. 84-WA/NCA-15.

Thomas, R.H., Burdisso, R.A., Fuller, C.R., and O'Brien, W.F., 1993, "Active Control of Fan Noise from a Turbofan Engine", AIAA paper no. 93-0597.

Tyler, J.M. and Sofrin, T.G., 1962, "Axial Flow Compressor Noise Studies", SAE Transactions, vol. 70, pp 309-332

Widrow, B., Glover, J.R., McCool, J.M., Kaunitz, J., Williams, C.S., Hearn, R.H., Zeidler, J.R., Dong, E., and Goodlin, R.C., 1975, "Adaptive Noise Cancelling: Principles and Applications", Proceedings of the IEEE, vol 63, no. 12, pp 1692-1716.

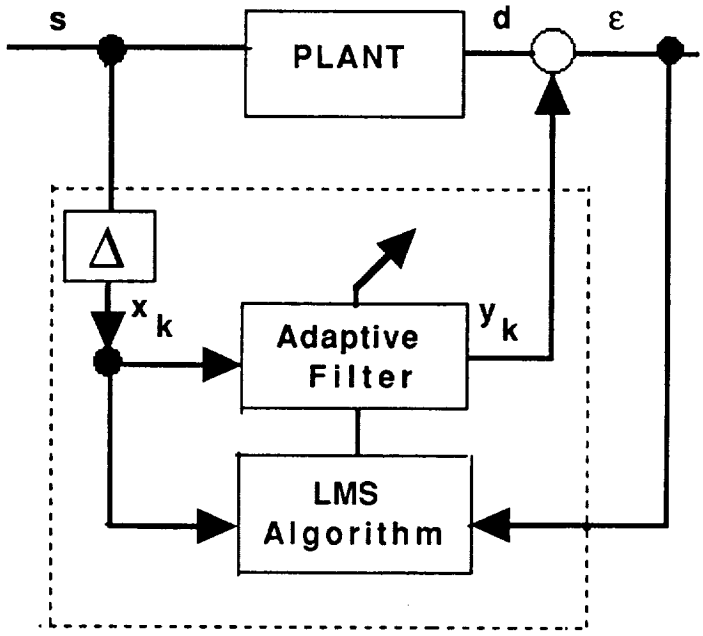

Figure 1. Generalized control system

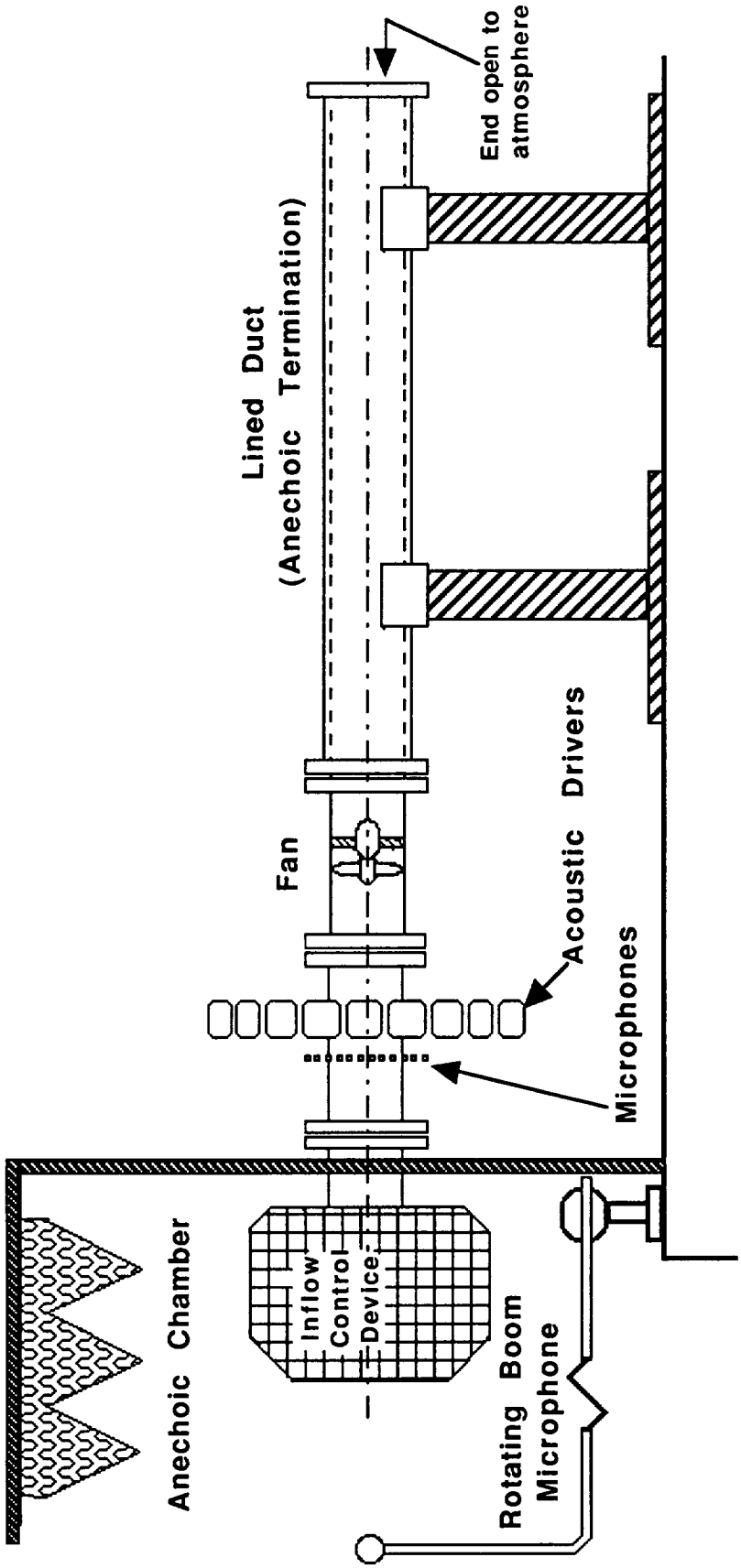

Figure 2. Fan noise control experiment layout

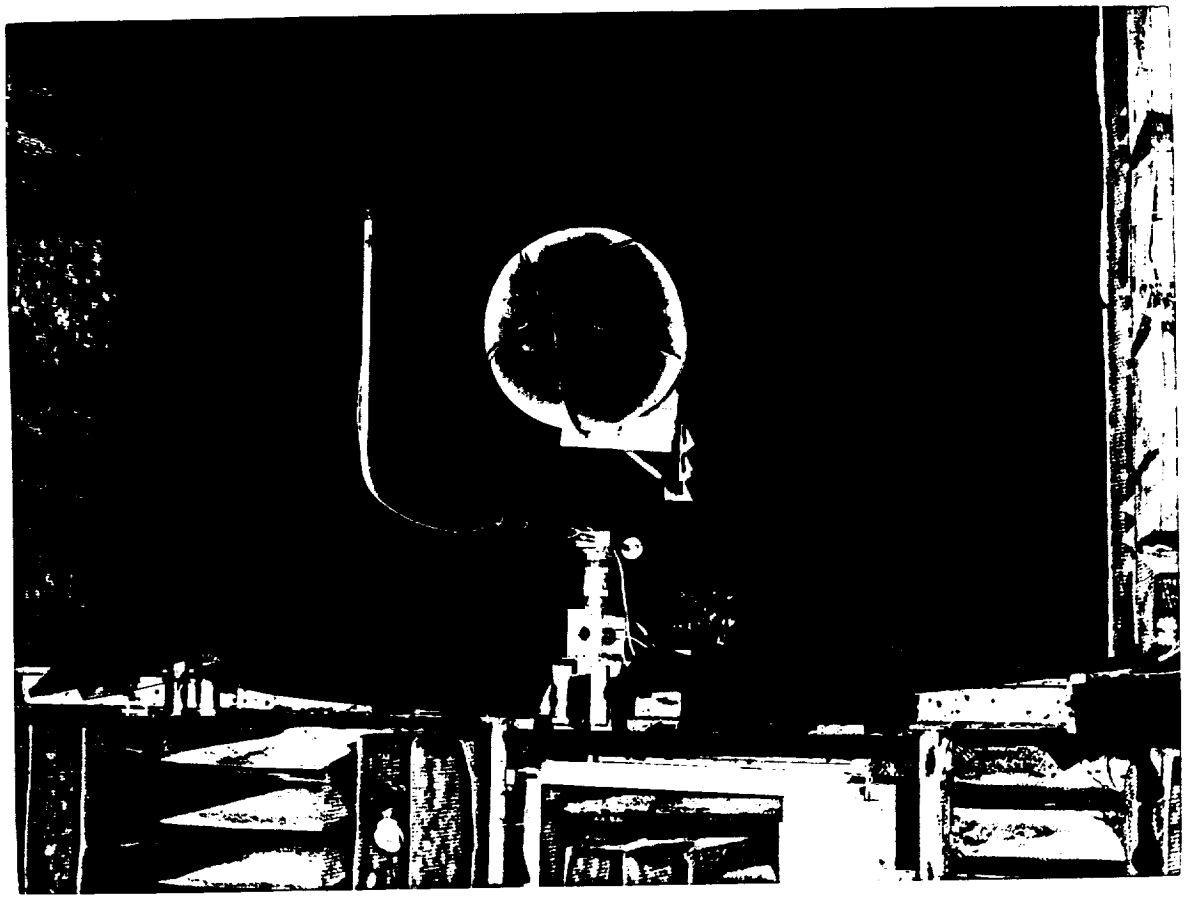

Figure 3. Fan Noise Control Ductwork, View from Inside the Anechoic Chamber showing Inflow Control Device and Far Field Microphone.

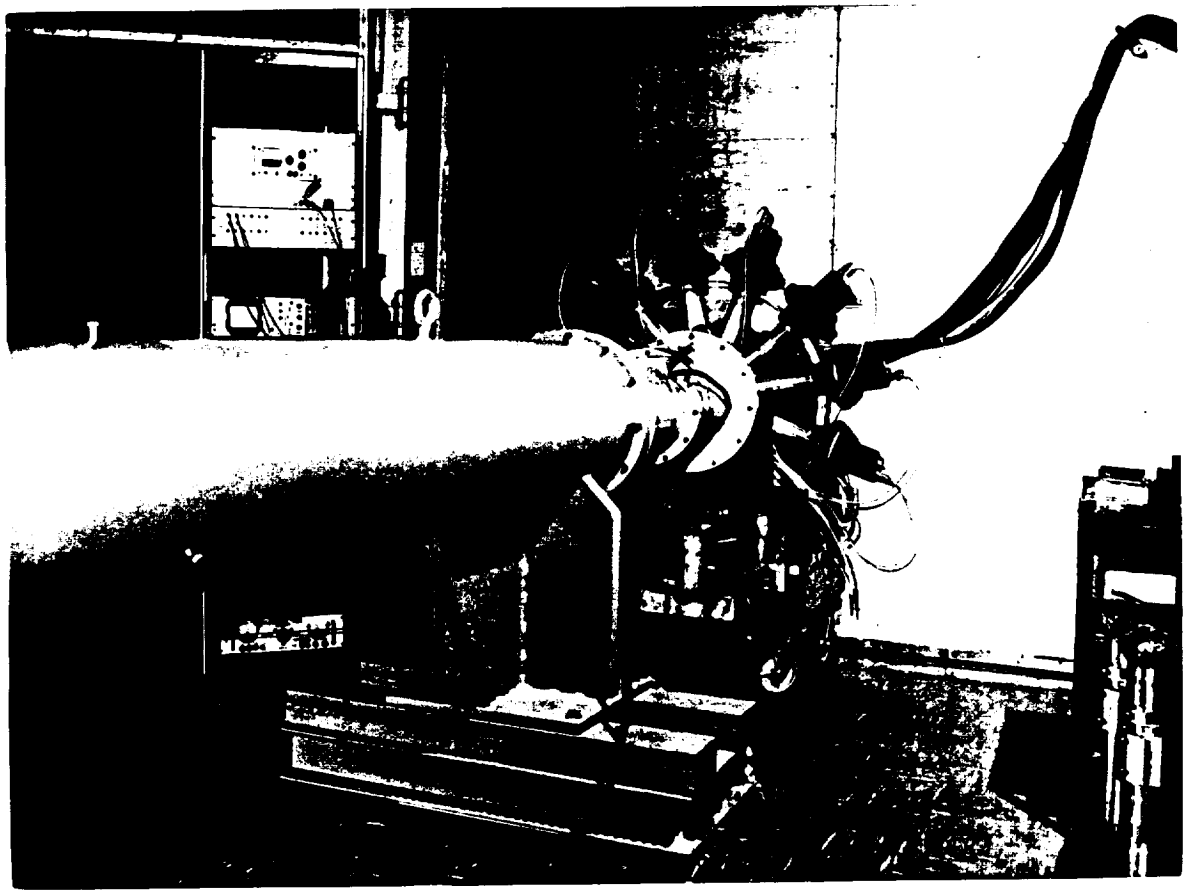

Figure 4. Fan Noise Control Ductwork, View from Outside the Anechoic Chamber Showing Noise Control Hardware, Fan, and Anechoic Termination Duct Sections.

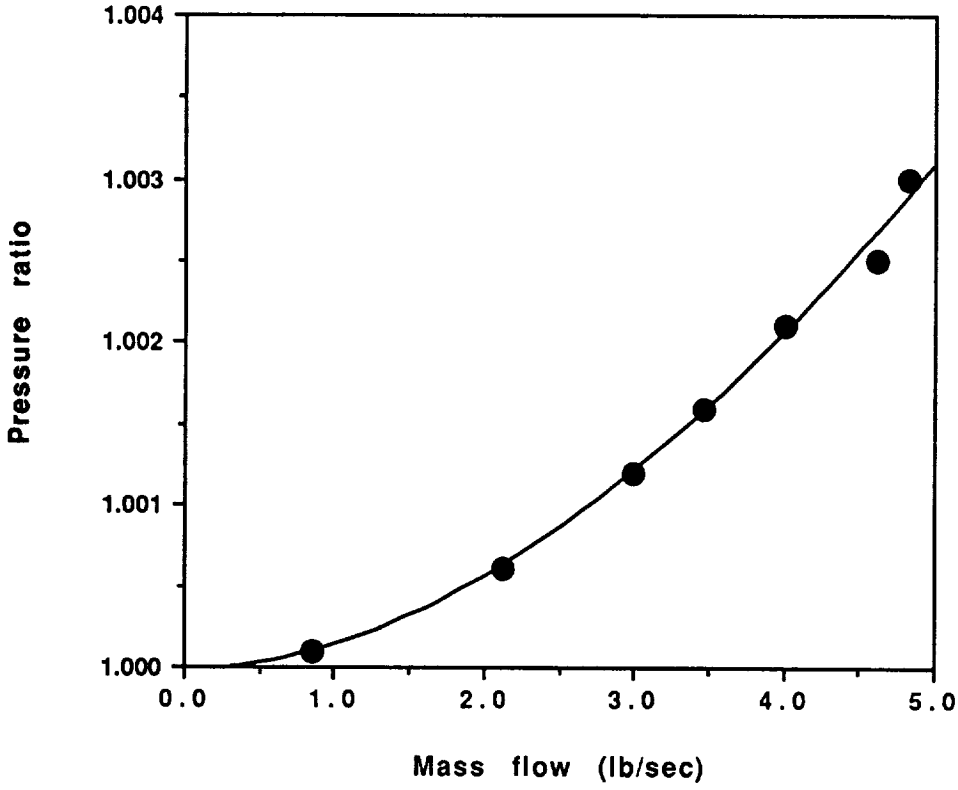

Figure 5. Ducted Axial Flow Fan Performance Curve

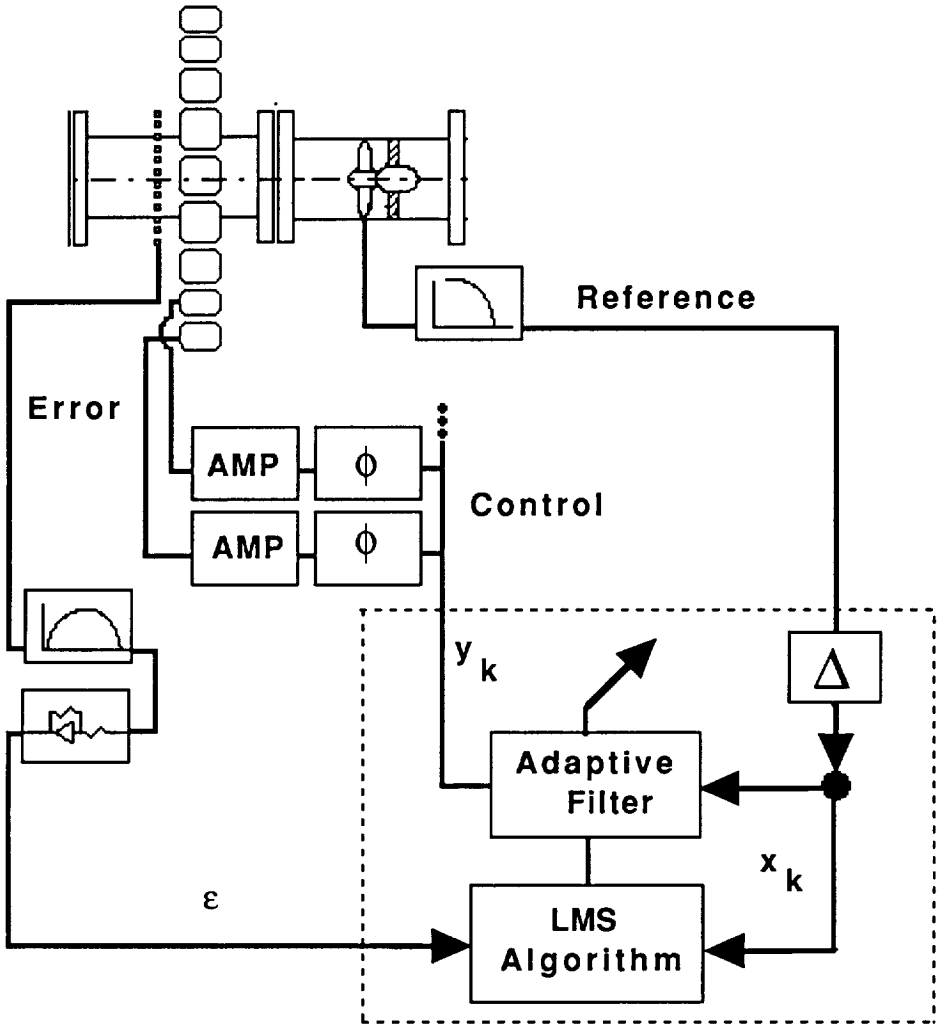

Figure 6. Fan noise control system setup

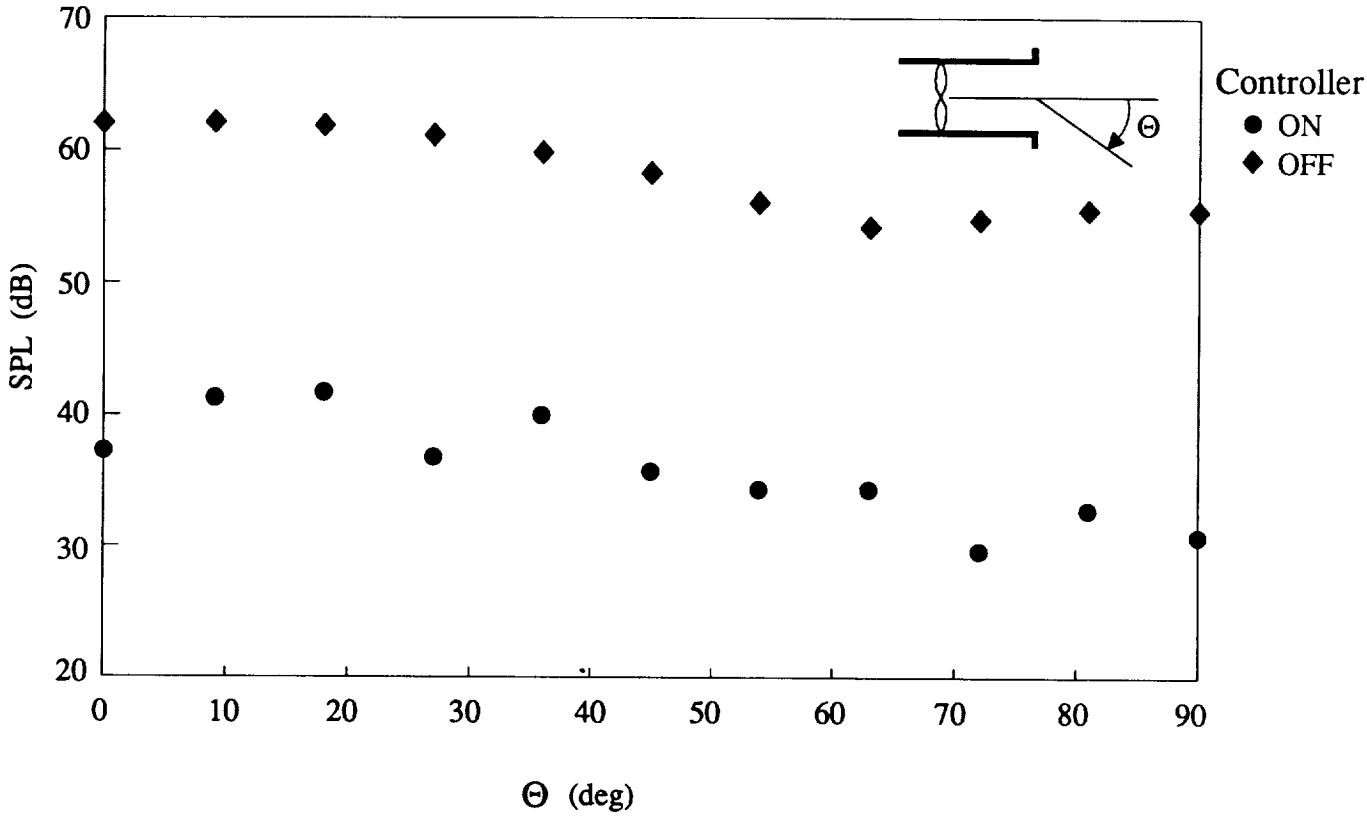

Figure 7.- Far field directivity of BPF tone with fan speed at 1500 rpm.

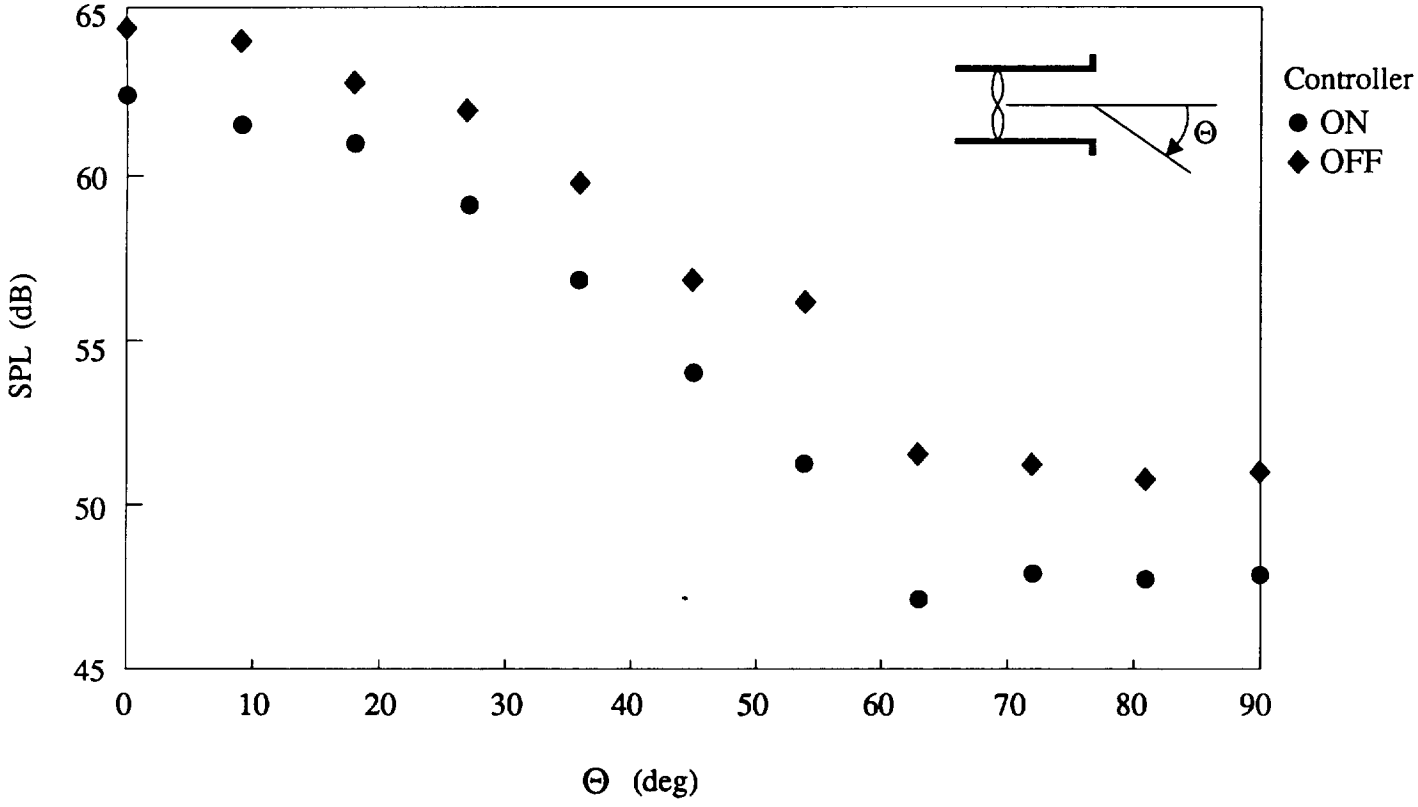

Figure 8.- Far field directivity of BPF tone with fan speed at 2700 rpm.

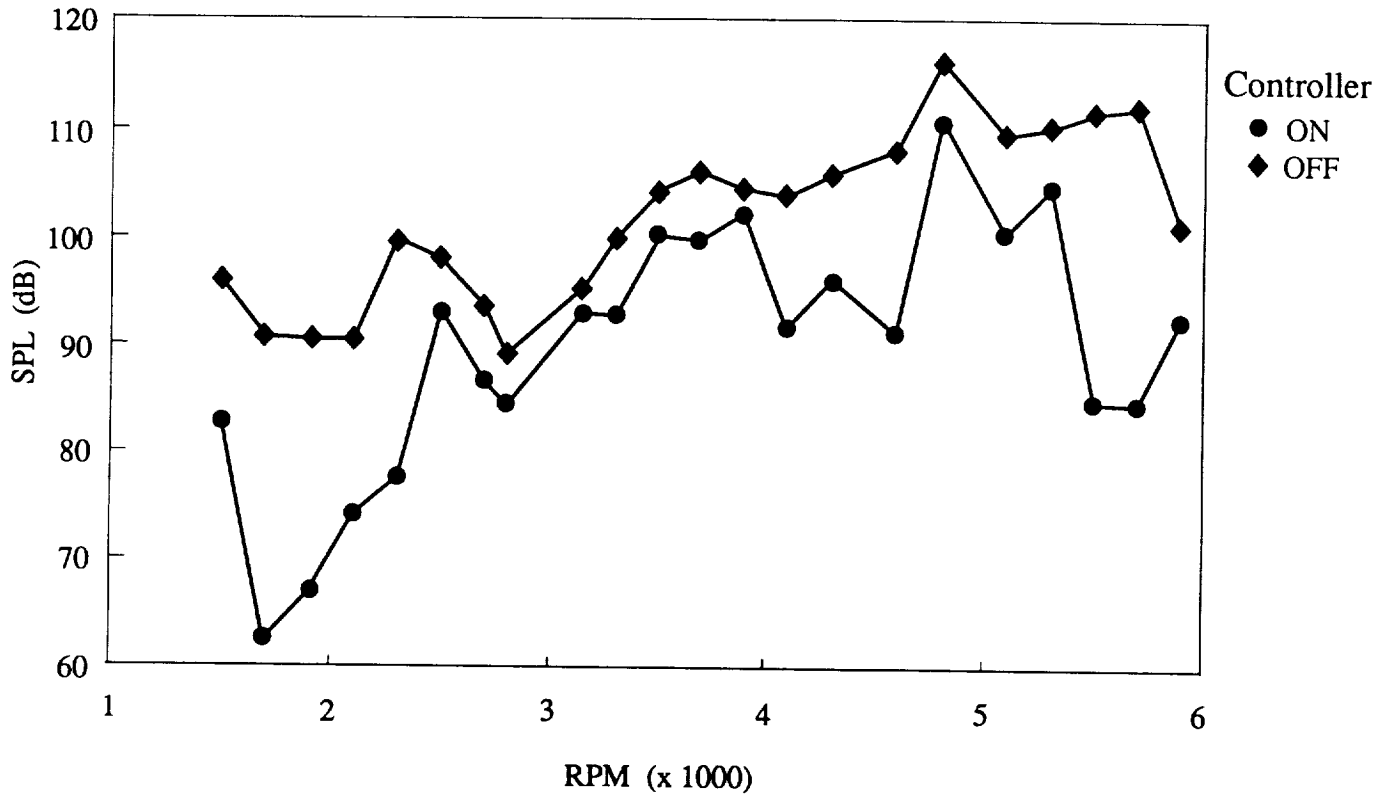

Figure 9.- Sound level spectrum of fan BPF tone at in-duct microphone.

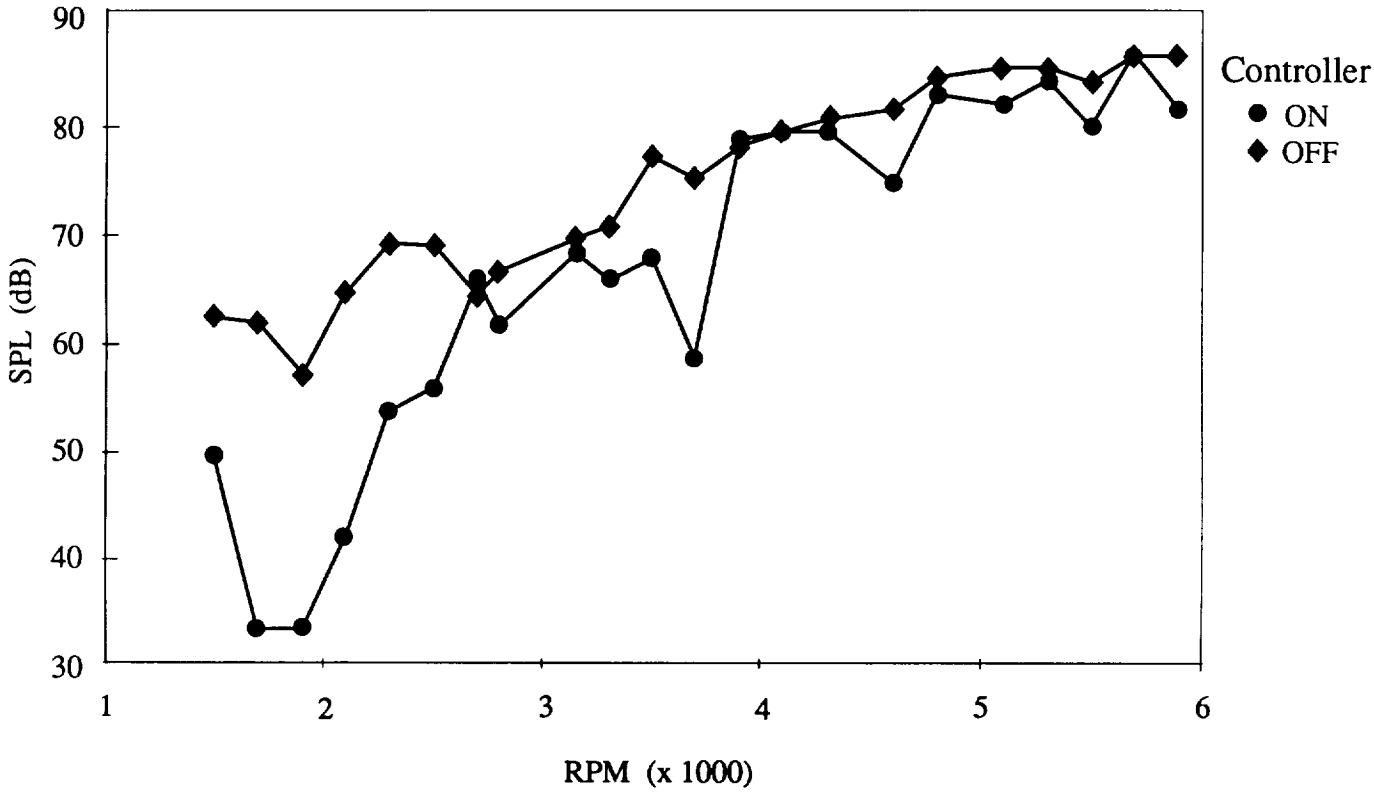

Figure 10.- Sound level spectrum of fan BPF tone at far field microphone.

REPORT DOCUMENTATION PAGE

Form Approved
OMB No. 0704-0188

1. AGENCY USE ONLY (*Leave blank*)	2. REPORT DATE	3. REPORT TYPE AND DATES COVERED
	August 1993	Technical Memorandum

4. TITLE AND SUBTITLE
Active Control of Fan-Generated Plane Wave Noise

5. FUNDING NUMBERS
WU 535-03-11-02

6. AUTHOR(S)
Carl H. Gerhold, William E. Nuckolls, Odillyn L. Santa Maria, and Scott D. Martinson

7. PERFORMING ORGANIZATION NAME(S) AND ADDRESS(ES)
NASA Langley Research Center
Hampton, VA 23681-0001

8. PERFORMING ORGANIZATION REPORT NUMBER

9. SPONSORING / MONITORING AGENCY NAME(S) AND ADDRESS(ES)
National Aeronautics and Space Administration
Washington, DC 20546-0001

10. SPONSORING / MONITORING AGENCY REPORT NUMBER
NASA TM-109008

11. SUPPLEMENTARY NOTES
Gerhold, Santa Maria, Martinson: Langley Research Center, Hampton, VA; Nuckolls: Analytical Services & Materials, Inc., Hampton, VA.

12a. DISTRIBUTION / AVAILABILITY STATEMENT
Unclassified - Unlimited

Subject Category 71

12b. DISTRIBUTION CODE

13. ABSTRACT (*Maximum 200 words*)

Subsonic propulsion systems for future aircraft may incorporate ultra-high bypass ratio ducted fan engines whose dominant noise source is the fan with blade passage frequency less than 1000 Hz. This low frequency combines with the requirement of a short nacelle to diminish the effectiveness of passive duct liners. Active noise control is seen as a viable method to augment the conventional passive treatments. This paper reports on an experiment to control ducted fan noise using a time domain active adaptive system. The control sound source consists of loudspeakers arrayed around the fan duct. The error sensor location is in the fan duct. The purpose of this experiment is to demonstrate that the in-duct error sensor reduces the mode spillover in the far field, thereby increasing the efficiency of the control system. In this first series of tests, the fan is configured so that predominantly zero order circumferential waves are generated. The control system is found to reduce the blade passage frequency tone significantly in the acoustic far field when the mode orders of the noise source and of the control source are the same. The noise reduction is not as great when the mode orders are not the same even though the noise source modes are evanescent, but the control system converges stably and global noise reduction is demonstrated in the far field. Further experimentation is planned in which the performance of the system will be evaluated when higher order radial and spinning modes are generated.

14. SUBJECT TERMS
Active noise control in ducts; Fan noise; Noise in ducts; Advanced ducted propeller engines

15. NUMBER OF PAGES
27

16. PRICE CODE
A03

17. SECURITY CLASSIFICATION OF REPORT	18. SECURITY CLASSIFICATION OF THIS PAGE	19. SECURITY CLASSIFICATION OF ABSTRACT	20. LIMITATION OF ABSTRACT
Unclassified	Unclassified		